Transactions of the KSNVE, 24(3) : 205~212, 2014
http://dx.doi.org/10.5050/KSNVE.2014.24.3.205

한국소음진동공학회논문집 제 24 권 제 3 호, pp. 205~212, 2014
ISSN 1598-2785(Print), ISSN 2287-5476(Online)

[Special Paper]

Flow and Flow Noise Analysis of HSM by Using CAA++

CAA++를 이용한 HSM에 대한 유동과 유동소음 해석

Young Nam Kim† and JunHee Chae*
김 영 남·채 준 희

(Received November 22, 2013 ; Revised January 22, 2014 ; Accepted January 22, 2014)

Key Words : CFD++, CAA++, NLAS(비선형 음향해석프로그램), Synthetic Turbulence Model(난류 가상모델), Sunroof Buffeting(썬루프 버페팅), Acoustic Locked Flow(음향장에 속박된 유동)

ABSTRACT

In this paper, sunroof buffeting analysis for Hyundai simple model(HSM) is studied computationally. For validation, the velocity profile of boundary layer around the opening of HSM was obtained and compared with experimental results. The analysis of sunroof buffeting is done in two parts. First a steady state solution is obtained using the Reynolds Averaged Navier Stokes (RANS) solver, and then the computed flow field information is used as input for CAA++. Second transient simulation by CAA++ is performed for the peak sound pressure levels and peak frequencies of buffeting noise over the ranges of flow velocities. The benchmark results of frequency and sound pressure levels showed the general phenomena and matched well with the experimental data obtained by Hyundai Motor Car.

요 약

이 연구에서 현대자동차의 단순실험모델(HSM)에 대한 썬루프 버페팅에 대한 수치해석이 수행되었다. 검증을 위하여 HSM 목부위의 경계층에 대한 속도분포 해석결과를 실험결과와 비교하였다. 썬루프 해석은 두 단계로 이루어졌다. 첫 번째로 난류 RANS 모델을 이용하여 정상상태 해석이 수행되었으며, 해석결과는 CAA++의 입력값으로 사용된다. 두 번째 단계는 유동속도에 대한 1차 최대 압력피크와 버페팅 주파수 해석을 위한 비정상상태 해석이 CAA++에서 이루어졌다. 주파수와 음향압력의 수치해석 결과는 타당한 물리적 현상을 보여주고 있으며, 현대 자동차의 실험결과와 잘 일치하는 결과를 보여주었다.

1. Introduction

Sunroof buffeting is typical example of cavity noise. The cavity noise is generated by coupling hydrodynamic self-sustained oscillation flows around the cavity opening which act as acoustic sources and acoustic modes which are generated in cavity as acoustic resonator. Hydrodynamic self-sustained oscillations of the separated shear

† Corresponding Author ; Member, Flow & Noise Inc.
E-mail : ynkim@flow-noise.co.kr
Tel : +82-2-2093-2972
* Flow & Noise Inc.

A part of this paper was presented at the KSNVE 2012 Annual Autumn Conference
‡ Recommended by Editor-in-Chief Weuibong Jung

layer near the opening of the cavity can excite the resonant acoustic modes of the cavity. Flow-acoustic resonance occurs when the frequency of the self-sustained shear layer oscillations is close to the acoustic resonant frequency of the cavity. High amplitude pressure oscillations and the formation of regular and distinct vortex structures are fundamental characteristics of the acoustic locked flows in the cavity.

In case of automobiles, it is generally known that buffeting frequency is about 25 Hz and sound pressure level(SPL) is above 100 dB.

In recent application, researchers are using computational aero acoustics(CAA) approach. But CAA simulation requires highly expensive and time-consuming computations on dense grid. CAA++ was developed to overcome these difficulties by Metacomp Technologies Inc, which is used in conjunction with computational fluid dynamics(CFD) to simulate unsteady flow and aeroacoustic noise. CAA++ can be applied to general aeroacoustic problems such as broad band noise, discrete tone noise and acoustic resonance problems. Furthermore, CAA++ can reduce computational times and enhance the accuracy by confining computational domain size near acoustic sources, using non-reflecting boundary conditions, coarse mesh and synthetic turbulence model.

The purpose of this study is to perform computational aeroacoustic simulations with HSM and compare the analysis results to the experimental results provided by HMC(Hyundai Motor Company). After validation of boundary layer velocity profile through the steady state simulation by CFD++, the present study investigates sunroof buffeting noise of HSM.

The cavity of HSM contains many acoustic absorbing materials in the interior, which Q-factor is very low compared with the cases of general cavities. But in this study, the prediction of the buffeting frequencies and the corresponding sound pressure levels(SPL) were simulated as the case of neglecting acoustic dissipation in the interior of HSM.

2. Benchmark Problem

All experiments for HSM have been performed in Hyundai Aeroacoustic Wind Tunnel. The dimensions of HSM are shown as illustrated in Fig. 1. Thick acoustic absorbing materials are adhered on all inner walls of HSM cavity for considering the same order of acoustic absorbing and dissipation effects as a real car interior. The details of the cavity opening are shown as Fig. 2.

The experimental tests were performed for following results.

• The boundary velocity profiles at hot-wire positions denoted with A, B and C as illustrated in

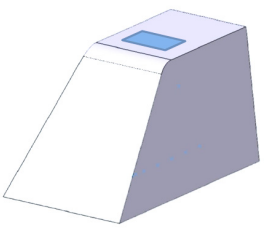

(a) HSM Geometry for sunroof buffeting test

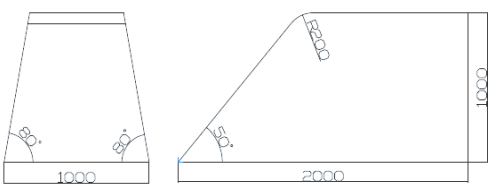

(b) Dimensions of HSM

Fig. 1 Geometries of HSM

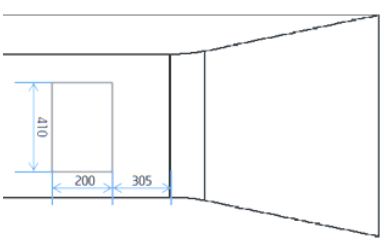

Fig. 2 Dimension of HSM opening

Fig. 3, when the cavity opening is closed. In this case, experiment is performed when flow velocity is 60 km/h.

• Frequency Response Test for estimating the acoustic resonance frequency and Q-factor of HSM cavity, when the cavity opening is opened and free stream velocity is 0 km/h.

• Sunroof buffeting SPL and frequencies over a range of flow velocities. In this case, frees stream flow velocities are 20, 30, 40, 50, 60, 70, 80, 90, and 100 km/h. The 1st peak SPL and frequencies are tested at the positions of microphone in Fig. 3.

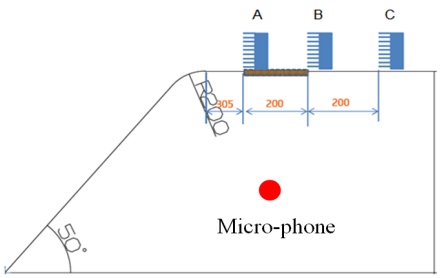

Fig. 3 Positions of hot-wire for boundary layer profile and microphone for sunroof buffeting

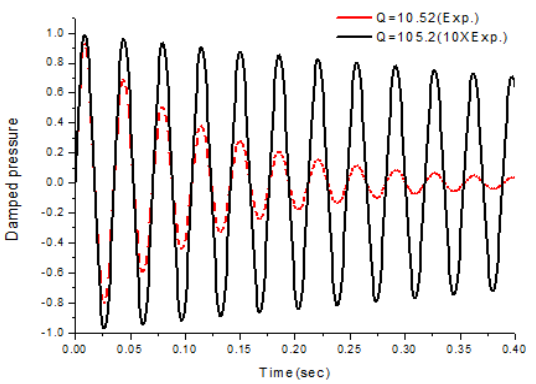

Fig. 4 Damped acoustic pressure in the cases of Q factor of 10.52 and 105.2

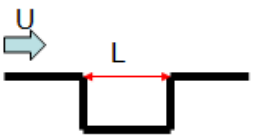

Fig. 5 Two dimensional simple cavity

The resonance frequency of 27.6 Hz and Q-factor of 10.52 are obtained by Frequency Response Test. Figure 4 shows the comparison with two Q-factors of 10.52 and 105.2, when cavity is analogized with a simple spring-mass system with the resonant frequency of 27.6 Hz. As shown in Fig. 4, HSM can be assumed as a high acoustic absorbing and dissipating system. In numerical analysis, failure to consider acoustic energy loss in the interior of HSM can be anticipated to result in many differences with experimental results from Fig. 4.

A simple cavity as illustrated in Fig. 5 is the practical example to estimate discrete tones related to fluid dynamic oscillation and flow modes generated around HSM opening. The frequencies of fluid dynamic oscillations are approximated by Rossister, 1964 in reference[3], as follows,

$$\frac{fL}{U_\infty} = \frac{n - \frac{1}{4}}{M_\infty + \frac{1}{k}} \tag{1}$$

where U_∞ is the free stream velocity and L is cavity opening length. The parameter k is empirically approximated to 0.56, which is the ratio of convective velocity to free stream velocity. Equation (1) calculates frequency of n^{th} mode based on the parameter n which can be approximated as the number of vortex near opening area. M_∞ is free stream Mach number and can be neglected because of $M_\infty \ll 1$.

Acoustic modes and acoustic resonant frequencies can be easily obtained from Helmholtz equations by numerical analysis with considering real geometries of HSM, in the form.

$$\left(\frac{2\pi f_m}{c}\right)^2 \Phi_m + \nabla^2 \Phi_m = 0 \tag{2}$$

Here Φ_m is m^{th} acoustic mode, f_m is m^{th} acoustic resonant frequency and c is the speed of sound. Acoustics modes of a cavity are a special

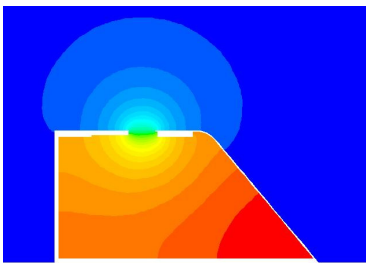

(a) Acoustic pressure contours of 1st mode

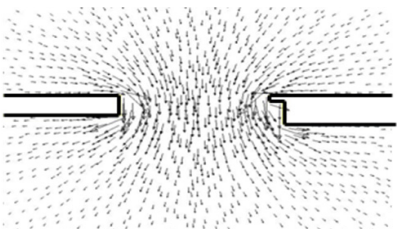

(b) Acoustic velocity vectors of 1st mode

Fig. 6 Acoustic 1st mode

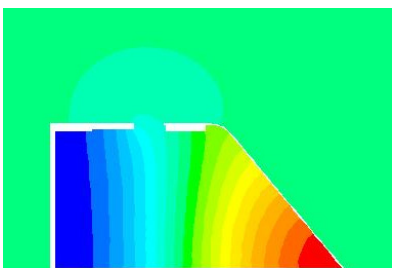

Fig. 7 Acoustic pressure of acoustic 2nd mode

case in which a standing wave is established near the mouth opening area and the interior of the cavity. Each acoustic frequency and acoustic mode is m^{th} eigenvalue and eigenvector of Helmholtz equation with homogeneous boundary conditions. The numerical method is explained in reference[2] in detail. In this study, the inverse power method was applied for this eigenvalue problem.

The 1st acoustic mode and acoustic velocities around HSM opening are shown in (a) and (b) of Fig. 6 and the second acoustic mode is illustrated in Fig. 7. The 1st acoustic resonance frequency was calculated as 28.3 Hz and the 2nd frequency as 104.1 Hz. As shown in (b) of Fig. 6, the flow of the 1st acoustic mode near the HSM opening

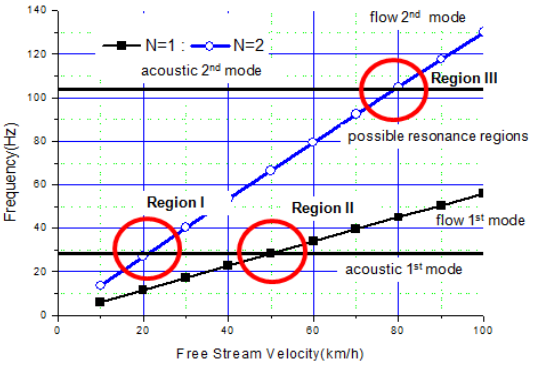

Fig. 8 Possible resonance regions

flows up and down according to acoustic pressure of the cavity interior.

At certain flow speeds, the vortex shedding frequency coincides with the acoustic resonance frequency of cavity. In this case, large pressure fluctuation is generated and the flow around opening area is strongly influenced by acoustic field. This state is known as acoustic locked flow. The typical phenomena of acoustics locked flow are large magnitude of unsteady pressure fluctuations above the dynamic pressure and periodic vortex formations as acoustic resonance frequency.

Figure 8 shows three possible resonance regions obtained from Eq. (1) and acoustic resonant frequencies as marked red circle. Possibilities to be several regions of acoustic locked flows in the cavity flows can be found in reference[1]. As shown Fig. 8, vortex shedding frequency increases according to the free stream velocity but acoustic resonant frequency is independent of flow velocities.

3. Numerical Analysis

3.1 Steady State

Steady compressible Reynolds averaged Navier-Stokes(RANS) equations are used to simulate the flow fields of HSM in commercially available solver CFD++(Metacomp Technologies). The two equation cubic k-turbulence model is

used for the steady RANS flows. This case was run on 4 processors using about the number of 1,200,000 meshes. The approximate turnaround time for this simulation was around 4 hours. The domain is decomposed into 4 parts to do parallel computations on 4 processors.

3.2 Transient Analysis

CAA++ non linear acoustic solver(NLAS) is used for the HSM buffeting noise simulations. The steady state solutions obtained from the steady state RANS by CFD++ is used to provide the initial conditions for unsteady calculation, the mean flow field, acoustic boundary conditions and turbulent statistics for the small scale turbulent acoustic source for NLAS simulations. In general, NLAS uses a confined computational domain by using non-reflecting boundary conditions because acoustic sources only exist around the cavity region.

NLAS is based on viscous non-linear perturbation equations made from compressible unsteady Navier-Stokes equations. Flow with large scale is calculated directly and smaller turbulent scales than grid size are modeled by the synthetic turbulent model (4). Detailed equations and explanations referring to NLAS are described in reference[4].

Pressure data at the location of microphone is recorded at every time step and then the 1st peak SPL and frequency are obtained from the acoustic pressure data. Fast Fourier transform(FFT) tool is used to get frequency spectrum from the simulated data.

SPL is defined as following relation. Here p is the perturbation amplitude and $p_{ref} = 2\times10^{-6}$ Pa.

$$SPL = 20Log_{10}\frac{p}{p_{ref}} \quad (3)$$

The time step for NLAS computation is set to be 3×10^{-4}, which provides sufficient stability on existing mesh and resolve all possible 1st and 2nd acoustic resonant frequencies.

The domain is decomposed into 4 parts to do parallel computations on 4 processors. This case was run on 4 processors by using about the number of 400,000 meshes. The approximate turnaround time for this unsteady simulation was around 48 hours.

4. Results & Discussions

The steady state results were obtained when free stream velocity 60 km/h. And the boundary layer velocity profiles are compared with the experimental results at the positions denoted in Fig. 3. Figure 9 shows the boundary layer mesh used for numerical analysis and the boundary layer velocity profiles compared with experimental results. All the numerical and experimental results show the boundary layer thickness increases according to distance from the beginning of HSM opening and numerical results predicts the boundary layer velocity profile with reasonable accuracy. Figure 10 shows the surface pressure and local velocity vectors around the front of HSM. The results show the strong vortex lines are formed near the front of HSM and A-pillar.

The 1st peak frequencies and SPL according to free stream velocities are compared with the experimental results supplied by HMC in Figure 11.

As the flow velocity is increased from zero, the peak SPL increase approximately linearly with flow velocity in all of the numerical and experimental results. The 1st peak SLP reach to the maximum value at the free stream velocity of 50 km/h in experimental results. And the SPL decreases as the flow velocity increases. But in the case of numerical results, the maximum 1st SPL was calculated at the free stream velocity of 60 km/h. The maximum SPL of numerical analysis was over estimated as the value of 135 dB which is 6 dB greater than the experimental results.

In current state, the main cause of this differ-

ence is attributed to simulation under the assumption which HSM is an un-damped system. The experimental results include the effects of the small Q-factor caused by large acoustic energy dissipation generated in the interior of HSM.

The acoustic locked flows are generated in wider range of velocities than the experimental results because of no considering the effects of small Q-factor. These phenomena are found in the un-damped system as reference[2]. (b) in Figure 11 compares the 1st peak frequencies of the experimental and numerical results. And (c) shows the 1st and 2nd peak frequencies in the interior of cavity and near the opening of the cavity.

All results of experiment and numerical simulation show only region II in Fig. 8 is activated as dominant acoustic locked flow over the range of flow velocities. But in flow velocity of 20 km/h or 30 km/h, a weak acoustic locked flow denoted as region I in Fig. 8 overlapped with the dominant acoustic locked flow can be anticipated because the frequencies of these ranges are close to 1st acoustic resonant frequency. This kind of example can be found in reference[1,2].

In the case of experiment, the 1st peak frequency at the free stream velocity of 20 km/h can be estimated to show the characteristics of the 2nd mode of flow. But the result of frequency at 30 km/h is attributed to abrupt change of the flow state from the 2nd to the 1st flow mode. In the case of numerical analysis compared with the experiment, the frequencies at these two velocities were predicted as the frequencies of the flow 2nd mode.

The 1st peak frequencies at the position of the microphone do not clearly show the natural frequency by Strouhal number. In the cases of flow velocity of 90 and 100 km/h, it is very difficult to define the flow state is the acoustic locked flow or not by only considering the frequency of the interior of cavity. But the peak frequency of the vortex shedding near the HSM opening precisely

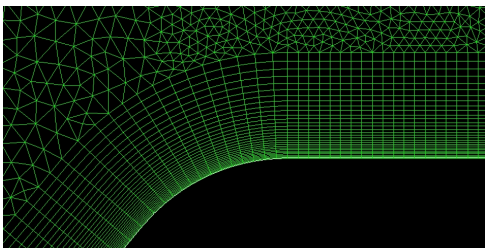

(a) Boundary layer mesh around the probe points

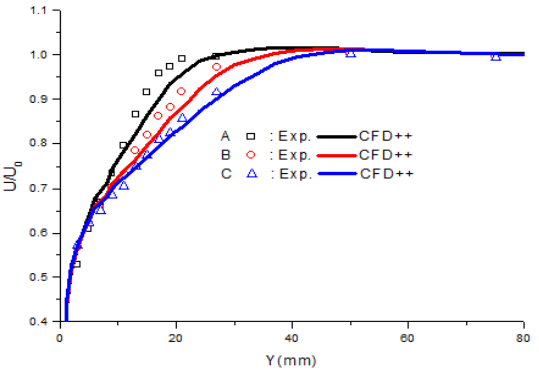

(b) Comparison between Numerical analysis and experimental results supplied by HMC

Fig. 9 Boundary layer velocity profile when flow velocity 60 km/h

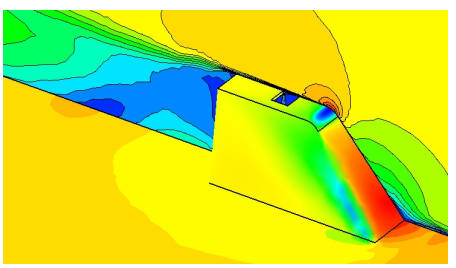

(a) Surface pressure and velocity contours in the symmetry plane

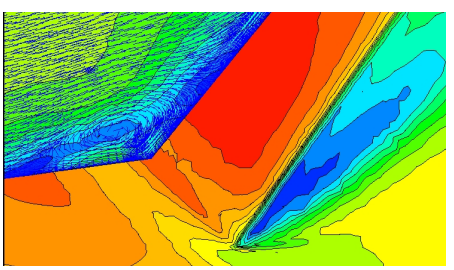

(b) Velocity vectors and detailed surface pressure contours

Fig. 10 Steady state flow results when flow velocity 60 km/h

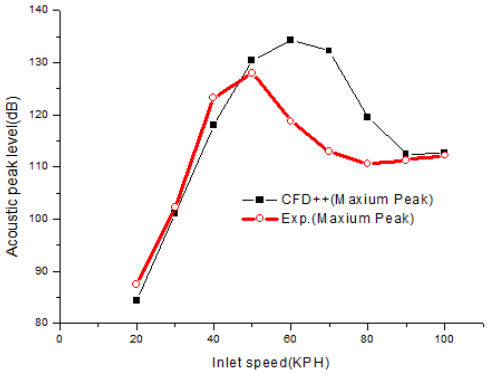

(a) Sound pressure level tested by HMC and the analysis results by CAA++

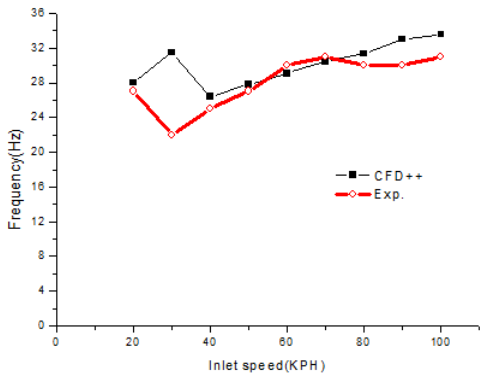

(b) 1st peak frequency tested by HMC and the analysis results by CAA++

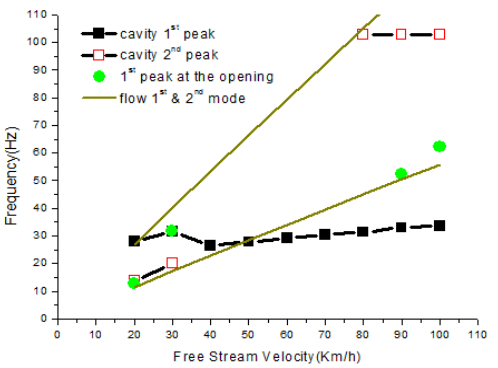

(c) 1st peak and 2nd peak frequency in Cavity and near the HSM opening by the analysis results by CAA++

Fig. 11 1st peak SPL and resonance frequencies

shows the Rossiter's relations as (c) in Fig. 11. In the case of numerical simulation, the flow state above the flow velocity of 90 km/h can be anticipated to escape from the influence of acoustic fields.

5. Conclusions

The acoustic resonant mode and frequencies was predicted by numerical analysis of Helmholtz equation. The acoustic resonant frequency was accurately estimated when compared to experiments. Flow natural frequency of the vortex shedding near the opening of HSM was estimated by theoretical approach considering a simple cavity model.

The map of acoustic resonant locked flow is suggested by using the numerical results of acoustic resonance mode and frequency, and Rossiter's relation. This map shows three resonant flow states are possible as increasing free stream velocity.

Steady state flow analysis was conducted for validation at the flow velocity of 60 km/h. the boundary layer velocity profiles are exactly predicted compared with the experiments.

In the transient analysis, the 1st peak SPL and frequencies in the position of microphone were compared with the experimental results. The maximum SPL is over predicted and the acoustic locked flows are estimated in more wide range of flow velocity compared with the experiments. The 1st peak frequency at the flow velocity of 30 km/h shows lower value than the experiment.

The cause of the difference between numerical and experimental results is attributed to simulation without considering the acoustic dissipation in the interior of HSM. But in this study, numerical results suggest the reasonable explanation of the buffeting process and acoustic locked flows for an undamped system.

Acknowledgments

We are thankful to HMC for supplying the experimental results in this study.

References

(1) Velikorodny, A., Yan, T. and Oshkai, P., 2010, Quantitative Imaging of Acoustically Coupled Flows Over Symmetrically Located Side Branches, Exp Fluids, 48:245-264.

(2) Stoneman, S. A. T., Hourigan, K., Stokes, A. N. and Welsh, M. C., 1988, Resonant Sound Caused by Flow Past Two Plates in Tandem in a Duct, J. Fluid Mech, Vol. 192, pp. 455~484.

(3) Rossister, J. E., 1964, Wind Tunnel Experiments of the Flow over Rectangular Cavities at Subsonic and Transonic Speeds, Aero. Res. Counc. R & M., 3438.

(4) Batten, P., Ribaldone, E., Casella, M. and Chakravarthy, S, 2004. Towards a Generalized Non-linear Acoustics Solver, AIAA 2004-3001, 10th AIAA/ CEAS Aeroacoustics Conference.

(5) CFD++ User Manual, Version 10.1.2, 2008. Metacomp Technologies, USA.

(6) Ryu, K. W. and Lee, J. S., 2002, Numerical Analysis of the Unsteady Pressure fluctuation Generated from the Interaction between a Vortex Flow with a Forward Step, Transactions of the Korean Society for Noise and Vibration Engineering, Vol. 12, No. 3, pp. 213~220.

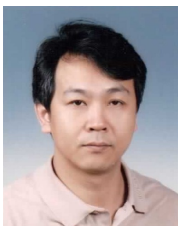

Young-Nam Kim received Ph.D. degree in Aerospace Engineering from Korea Advanced Institute of Science and Technology in 2012. He is the CEO of Flow&Noise Inc. and he has been working in the field of CFD and CAA since 1995.

Jun-Hee Chae received M.A. degree in Mechanical Engineering from Korea Aerospace University in 1996. He is working as the Technical Support Manager of Flow&Noise Inc. and he has been working in the field of CFD since 1996.